13th Australasian Fluid Mechanics Conference
Monash University, Melbourne, Australia
13-18 December 1998

NUMERICAL SIMULATION OF DROPLET IMPACT ON A HIGH TEMPERATURE SOLID SURFACE

Dalton J.E. HARVIE[1] and David F. FLETCHER[2]

[1]Department of Mechanical and Mechatronic Engineering
and
[2]Department of Chemical Engineering
University of Sydney, NSW, AUSTRALIA

ABSTRACT

A numerical code, BOUNCE, is presented to simulate the non-wetting impact of droplets on high temperature surfaces. The code is composed of a VOF (Volume of Fluid) solution to flow within the droplet, coupled to a one dimensional solution of flow within the viscous vapour layer. A direct comparison with an experimentally observed impact shows that the code predicts the dynamics of the droplet well.

INTRODUCTION

Water droplets are used as an efficient method of solid cooling in a wide variety of applications, including emergency nuclear reactor core cooling, annealing of metals and in the suppression of pyrolysis from burning solids. While the dynamics and heat transfer from droplet impacts has undergone substantial experimental research, little analytical work has been conducted into droplet dynamics within the non-wetting Leidenfrost regime.

Among the large number of experimental studies is the work of Wachters and Westerling (1965). Here, water droplets of initial diameter 2.3mm were projected at a polished gold surface. The droplet temperature was initially at saturation and the dynamics of impingement were captured in a series of photographs. Heat transfer from droplets at different impact velocities and diameters was also studied.

More recently, Chandra and Avedisian (1991) fired n-heptane droplets of initial diameter 1.5mm at a polished stainless surface. The temperature of the surface was varied from room temperature to well above the Leidenfrost point, and the dynamics of droplet behaviour was captured in another series of excellent photographs.

The purpose of this work is to simulate the dynamics of droplet impingement on a high temperature solid surface. Specifically, the solid temperature is high enough that wetting does not occur, the solid is assumed perfectly smooth, and no subcooling of the droplet is allowed.

NUMERICAL MODEL

Simulations are performed by coupling a viscous vapour layer flow between the solid and droplet to a full Navier-Stokes solution of flow within the droplet.

Droplet Solution

BOUNCE is based on the well documented SOLA-VOF (Nichols, Hirt and Hotchkiss, 1980) code, although significant changes have been made to suit this application and to reflect advances in simulation techniques over the past decade.

Fluid flow within the droplet satisfies the incompressible continuity equation and the full Navier-Stokes equations in two dimensional cylindrical coordinates,

$$\frac{1}{r}\frac{\partial(ru)}{\partial r}+\frac{\partial v}{\partial z}=0, \tag{1}$$

$$\frac{\partial u}{\partial t}+u\frac{\partial u}{\partial r}+v\frac{\partial u}{\partial z}=-\frac{1}{\rho}\frac{\partial p}{\partial r}+\frac{F_r}{\rho}+\upsilon\left[\frac{\partial^2 u}{\partial r^2}+\frac{\partial^2 u}{\partial z^2}+\frac{1}{r}\frac{\partial u}{\partial r}-\frac{u}{r^2}\right], \tag{2}$$

$$\frac{\partial v}{\partial t}+u\frac{\partial v}{\partial r}+v\frac{\partial v}{\partial z}=-\frac{1}{\rho}\frac{\partial p}{\partial z}+\frac{F_z}{\rho}+\upsilon\left[\frac{\partial^2 v}{\partial r^2}+\frac{\partial^2 v}{\partial z^2}+\frac{1}{r}\frac{\partial v}{\partial r}\right], \tag{3}$$

where $$\rho = f\rho_f . \tag{4}$$

The radial and vertical components of the fluid velocity are u and v respectively, while F_r and F_z are the components of the body force comprising gravity, the volume surface tension force and volume vapour layer force, as discussed below. The density of the liquid is ρ_f, and the Volume of Fluid (VOF) function, f, defines the proportion of cell volume occupied by fluid. Advection of f is governed by,

$$\frac{\partial f}{\partial t}+u\frac{\partial f}{\partial r}+v\frac{\partial f}{\partial z}=0. \tag{5}$$

The equations are discretized on an Eulerian rectangular mesh, and solved using an incomplete Cholesky conjugate gradient (ICCG) matrix inverter (Kothe and Mjolsness, 1992, Kuo-Petravic and Petravic, 1981).

Surface Tension is calculated using the Continuum Surface Force (CSF) model of Brackbill, Kothe and Zemach (1991). Under this model, discrete pressure jumps occurring at fluid surfaces are replaced by a continuous volume force which acts everywhere on the fluid within a transition region surrounding the surface. Such a model is ideally suited to the VOF technique, and the present implementation follows that of the Ripple VOF code (Kothe and Mjolsness, 1992).

Viscous Vapour Layer

Figure 1 shows the variables used in calculating the flow within the vapour layer. Several assumptions have been employed:-

1) The temperature of the liquid at the top of the layer (ie the droplet temperature) is constant and equal to saturation temperature at atmospheric pressure. Numerical results show that peak relative pressures within the layer are of the order of 10kPa. This increase in pressure corresponds to an approximately 10K increase in the saturated liquid temperature for water. This is probably very significant, but at present we assume saturation for simplicity.
2) The temperature of the solid surface is constant. While this assumption may be relaxed in future studies, it is justifiable for use with high thermal diffusivity solid surfaces.
3) The size of molecular layers at both droplet surface and solid surface are very small, thus the vapour temperature at the top of the layer equals the droplet temperature, and the vapour temperature at the bottom equals the solid temperature.
4) The vapour layer contains only water vapour. This assumption will be relaxed in the future to allow simulation of droplet impacts in mixtures of air and steam, but is used here for simplicity.
5) The properties of the vapour are constant, and equal to properties of steam at the average vapour temperature and atmospheric pressure.
6) The reactive force resulting from liquid vaporisation on the underside of the droplet is neglected. The magnitude of this force is much lower than the force resulting from viscous flow within the layer.
7) The layer has a height significantly smaller than its radius, so that the magnitude of the vertical component of the vapour velocity is assumed negligible in comparison with the horizontal component.
8) Heat transfer to the droplet from the solid is dominated by one dimensional conduction.

These last two assumptions are consistent with the work by Gottfried, Lee and Bell (1966) on the vaporisation of stationary Leidenfrost droplets.

A mass balance of fluid within the layer is performed by considering a fluid mass balance on a cylinder of radius r', as shown in figure 1. Thus

$$\overline{u}_v(r') = \frac{1}{r'\delta(r')}\int_0^{r'}\left(\frac{k_v(T_s - T_d)}{\delta(r)h_{fg}\rho_v} - \frac{d\delta}{dt}(r)\right)r\,dr, \quad (6)$$

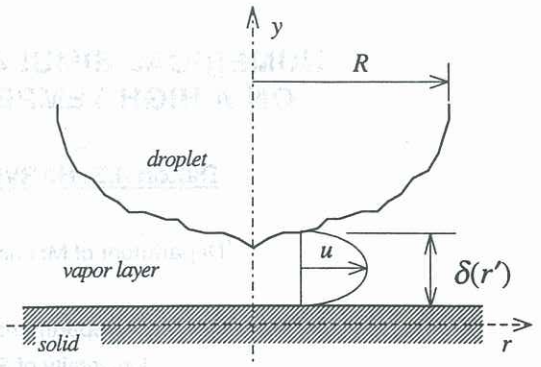

Figure 1: Variables used in viscous vapour layer.

where $\overline{u}_v(r')$ is the radial velocity [m/s] of the vapour averaged across the height of the layer, ρ_v is the density of the vapour [kg/m^3], k_v is the thermal conductivity of the vapour [W/m.K], T_s and T_d are the solid surface and droplet temperatures [K] respectively, $\delta(r)$ is the height of the vapour layer as a function of radius [m] and h_{fg} is the latent heat of vaporisation of water plus the sensible heat [J/kg].

Employing the previous vapour layer assumptions, the Navier-Stokes equation in the radial direction simplifies to a viscous flow equation. Integrating twice in the vertical direction, noting that the vapour velocity at the top and bottom of the layer is zero, and averaging over the height of the layer (Gottfried, Lee and Bell, 1966) gives

$$\overline{u}_v(r') = -\frac{\delta(r')^2}{12\mu_v}\frac{\partial P_v(r')}{\partial r'}. \quad (7)$$

Integrating again in the radial direction, using the assumption that the relative pressure within the vapour layer (P_v) is atmospheric at the maximum radius of the droplet (R), the pressure within the vapour layer is found in terms of the average vapour velocity and the geometry of the layer,

$$P_v(r') = -12\mu_v\int_R^{r'}\frac{\overline{u}(r)}{\delta(r)^2}\partial r. \quad (8)$$

Equations (6) and (8) are integrated numerically to find the viscous vapour layer pressure in each computational fluid cell acting on the base of the droplet. This pressure is reformulated as a surface volume force, in a manner analogous to the surface tension volume force, and substituted back into the main VOF code.

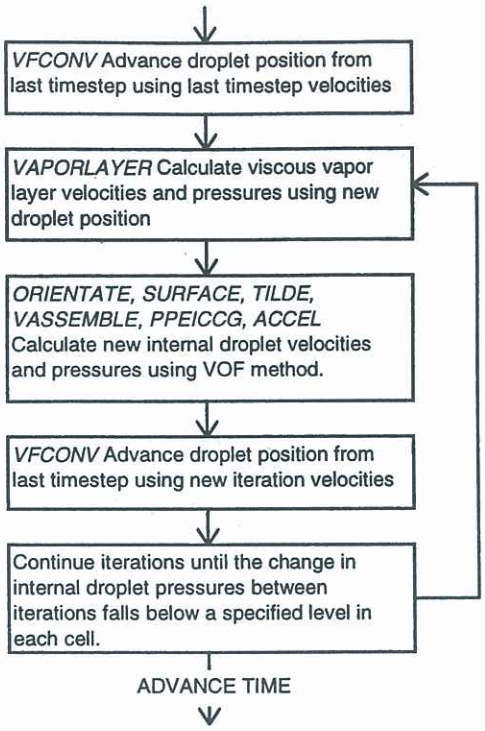

Figure 2: Schematic diagram of implicit surface treatment iterative method used to advance the solution.

Implicit Surface Treatment

An implicit treatment of the position of the droplet surface was required as the vapour pressure is critically dependent on the accurate calculation of the lower surface of the droplet. Figure 2 schematically shows how these implicit iterations were performed at each timestep.

EXPERIMENTAL COMPARISON

Figure 3 shows a comparison between an actual water droplet impact as photographed by Wachters and Westerling (1965) and a cross-section of the same impact as generated by BOUNCE. The example was chosen because it most closely resembles conditions existing in our numerical model. Specifically,

1) the impact surface was gold, a material of high thermal diffusivity with a large characteristic thermal diffusion length ($2\sqrt{\alpha t}$) over the duration of the impact of 2.8mm, thus approximating our infinite thermal diffusivity of solid model,
2) the droplet was initially heated to 100°C, consistent with our constant saturation temperature droplet assumption, and
3) impacts occurred in an atmosphere of steam, consistent with our assumptions, and also ensuring that the droplet temperature remained close to saturation between projection and impact.

The droplet had an initial undeformed diameter of 2.3mm, Weber number of 15, and a corresponding impact velocity of 0.70 m/s. The temperature of the surface was 400°C.

The numerical simulation was calculated using a 50×140 grid over a computational domain of 0 to 2.5mm radially and -0.15 to 6.85mm vertically. The code took approximately 4000 timesteps to complete 18ms of simulation, giving an average timestep of 4.5μs. Such a small timestep is a result of the inherently stiff nature of the physical problem. As the computation was performed in cylindrical coordinates, an axis of symmetry was implemented for the left boundary. In producing the surface contour plots of figure 3, the images were reflected around the centreline.

BOUNCE predicts the behaviour of the droplet well. The first four frames, up to 1ms, display the initial impact of the droplet. As shown in the generated images, upon impact, a wave of water at the bottom surface of the droplet moves radially outward from the centre. The crest of this wave is very close to the solid, but with increasing distance from the centre, moves slightly upward. Due to the reflection of light off the photographed droplet, it is not possible to compare directly the behaviour of the droplet base within the vapour layer. However, consistent with the simulation, the photographs do show that the vapour layer height is very small at the extremity of the layer.

The next five frames, from 1 to 4 ms, show the droplet spreading out over the surface. By this stage, in both the computations and photographs, the thickness of the vapour layer has increased to a visible level. The computations show that from frames seven and onwards, smaller secondary waves occur at the base of the droplet and move outward from the centre like the impact wave.

There appears to be an internal central hump of fluid shown in photograph nine (3.85ms) of the experimental impact. Computations showed that between 3.5 and 6 ms, the geometry of the central region of the droplet changed quite substantially and quickly. Whilst the computed droplet displays a smaller central hump, it must be noted that the frame times between the experimental example and simulation do not correlate exactly.

Frame ten (5.44ms) shows that the computational droplet splits into a toroid and central droplet before rebounding. It is not entirely clear whether this occurs in the experimental case, but the real droplet does have a larger radius at the top of the central region. This may suggest that the computational surface tension method is slightly underestimating the real surface tension force.

The last six frames, from 6ms onwards, show the droplet recollecting as it is pushed away from the surface. During this period the vapour layer is quite oscillatory, becoming thin in places. BOUNCE predicts the droplet recoil process well, particularly the dumbbell shape shown in the final photograph and computational frame.

Computations were continued past the last experimental photograph for a further 3ms. These showed that the dumbbell shown at 14.7ms reforms into one oscillating droplet within a few milliseconds.

It should be noted that the photographs are a record of just one droplet impact, and as such not an average of how all similar droplets behave. In future work, comparisons with heat transfer rates and rebound velocities, both of which are easily averaged over several experimental impacts, will also be presented.

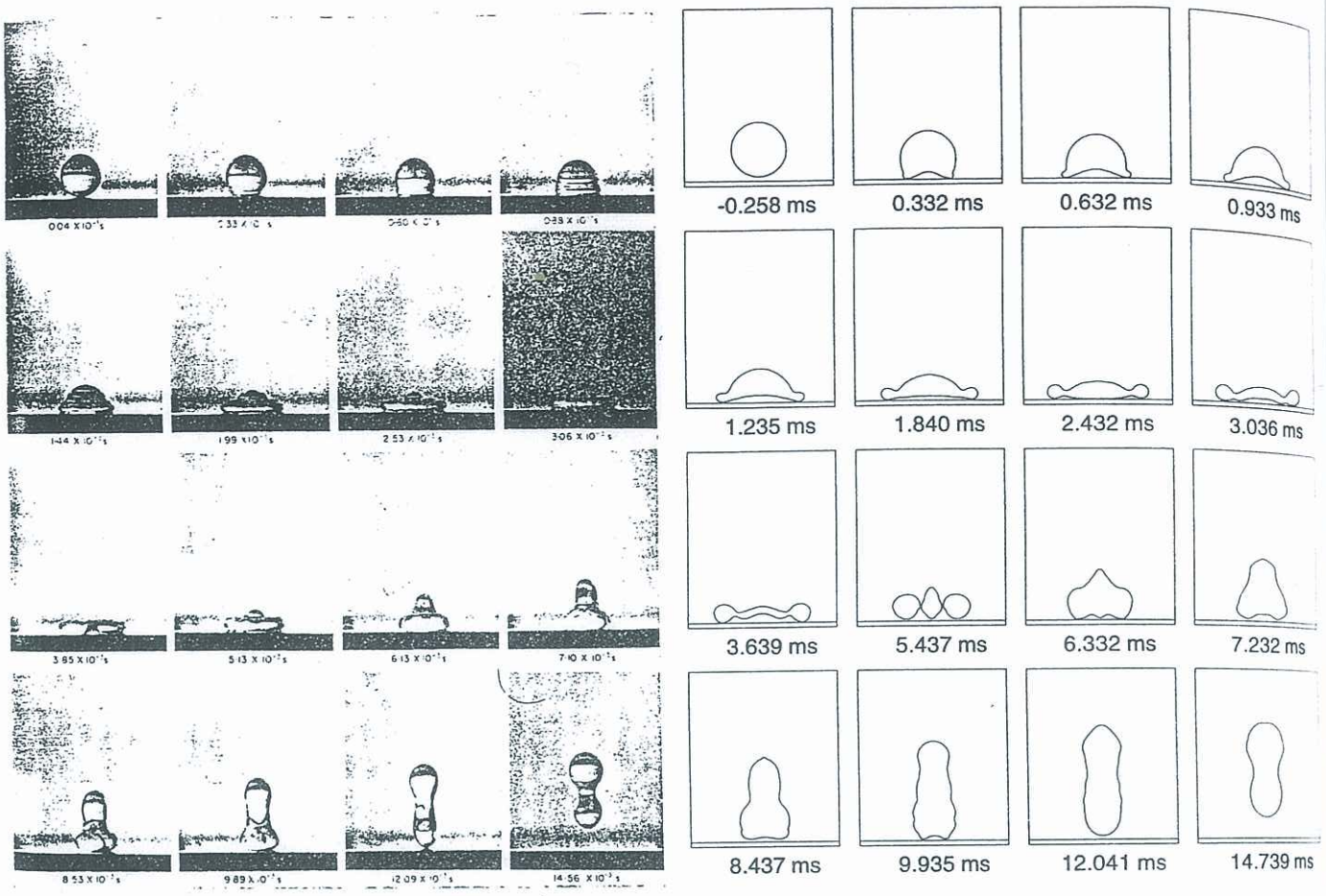

Figure 3 : Photographs of Wachters and Westerling (1965) impact and images of comparable BOUNCE impact.

CONCLUSION

The BOUNCE code predicts the behaviour of an impacting droplet well. While there are small differences between an examined computational and experimental droplet impact, BOUNCE predicts the residence time of the droplet on the surface and the qualitative geometry of the droplet accurately. Any small differences between cases could simply be due to the compared experimental impact differing from the experimental mean behaviour.

Future work will investigate heat transfer within the solid, especially relevant to low thermal conductivity surfaces such as wood, and heat transfer to the droplet. This will include an analysis of droplet subcooling, which is prevalent in almost all industrial and fire safety applications. Further work will examine solid porosity.

REFERENCES

BRACKBILL, J.U., KOTHE, D.B. and ZEMACH, C., "A continuum method for modeling surface tension", *J. Comp. Phy.*, **100**, 335-354, 1992.

CHANDRA, S. and AVEDISIAN, C.T., "On the collision of a droplet with a solid surface", *Proc. R. Soc. Lond. A*, **432**, 13-41, 1991.

GOTTFRIED, B.S., LEE, C.J. and BELL K.J., "The Leidenfrost phenomenon: film boiling of liquid droplets on a flat plate", *Int. J. Heat Mass Transfer*, **9**, 1167-1187, 1966.

GROENDES, V. and MESLER, R., "Measurement of transient surface temperatures beneath Leidenfrost water drops", *Heat Transfer*, **4**, 131-136, 1982.

KOTHE, D.B. and MJOLSNESS, R.C., "RIPPLE: a new model for incompressible flows with free surfaces", *AIAA J.*, **30**:11, 2694-2700, 1992.

KUO-PETRAVICK, G. and PETRAVICK, M., "A program generator for the incomplete cholesky conjugate gradient (ICCG) method with a symmetrizing preprocessor", *Comp. Phy. Com.*, **22**, 33-48, 1981.

NICHOLS, B.D., HIRT, C.W. and HOTCHKISS, R.S., "SOLA-VOF: a solution algorithm for transient fluid flow with multiple free boundaries", *LA-8355*, Los Alamos Scientific Laboratory, University of California, 1980.

WACHTERS, L.H.J. and WESTERLING, N.A.J., "The heat transfer from a hot wall to impinging water drops in the spheroidal state", *Chem. Eng. Sci.*, **21**, 1047-1056, 1966.